International Journal of Engineering Research Updates

Journal homepage: https://orionjournals.com/ijeru/

ISSN: 2783-0187 (Online)

(RESEARCH ARTICLE)

Check for updates

Numerical simulation study of nozzle bench mark axial velocity before sudden expansion using computational fluid dynamics

Thomas Okechukwu Onah *, Onyekachi Marcel Egwuagu and Chidiebere Diyoke

Mechanical and production Engineering, Enugu state university of Science and Technology, Enugu State, Nigeria.

International Journal of Engineering Research Updates, 2022, 03(01), 011–024

Publication history: Received on 08 May 2022; revised on 30 June 2022; accepted on 02 July 2022

Article DOI: https://doi.org/10.53430/ijeru.2022.3.1.0040

Abstract

Food and drug administration (FDA) benchmark study for biomedical flow transition. An idealized medical device is presented and CFD predictions of pressure and velocity are compared against experimental measurements of pressure and velocity. The fluid flow transitions considered laminar (Re=500), transitional (Re =2000), and turbulent (Re=6500) with various turbulence fluid flow simulation models of laminar, k-omega, k-omega SST and k-epsilon based on inlet throat Reth. = 500, 2000 and 6500. Axial velocity at centreline for Reth = 500, 2000 and 6500 at line X =0, showed maximum difference of 77.4% for velocity at centerline at 0.08m and 19% for wall pressure at -0.09m sudden expansion at laminar region of Re = 500. Good agreement with simulation happened at 65.6% and 17.2% transition Re =2000. At turbulent region Re = 6500, all models were in good agreement at 49.6% velocity centerline and 8.10% pressure drop, But in laminar legion, downstream of the simulation of Reth =6500, other models disappeared which demonstrated K-epsilon model is best at higher Reynolds turbulent region. Emphatically, from 0 to -120N/m2 counterbalanced at Reth = 500 wall pressure showed negligible axial pressure gradient at centerline with drop in normalization point of experimental data.

Keywords: Sudden Expansion; Axial Velocity; Simulation; models; computational Fluid Dynamics; Bench Mark

1 Introduction

In biomedical applications, CFD is used in designing and analyzing medical device, it can help with visualization of a particular problem, and provide insight into patterns within a flow field. However, the practice of using CFD simulations in assessing viability of medical devices is not well established. As such U.S. Food & Drug Administration (FDA) have designed a computational inter laboratory study (with 28 independent groups) to validate CFD techniques and produce experimental parameters to support CFD verification and validation (Huang, 2018). The thesis therefore focuses on evaluating CFD performance of Nozzle Benchmark of 2D axisymmetric model using Simulation models for prediction blood fluid flow transition for FDA which is one out of numerous techniques of solving numerical problems of Navier-Stokes equations (NSE), in the fluid dynamics areas have found it need in biomedical area (Bernsdorf et al., 2008), (Jain et al., 2017); (Munn, 2008); and (Jain, 2020). This technique represents and handle complex anatomical geometries with ease and also enable simulations on massively parallel computing architectures (Jain et al., 2017). (Jain, 2020), (Zhang et al., 2008), (Jain et al., 2017) have been applied in LBM for complex transitional flows of anatomical geometries and found efficient and effective. However, effort has not been made to appraise its effectiveness in FDA nozzle benchmark area. It is overbearing, to discover suitability of benchmark using methods without application (White & Chong, 2011). LBM application to FDA nozzle benchmark was only for laminar cases. Previous works done on computation transition flow using LBM was for moderate Reynolds number by (Jain, 2020) and (Jain et al., 2017). Therefore, there is need to evaluate simple LBM scheme, without employing complex collision synthetic models at turbulence inflow, to accurately

* Corresponding author: Thomas Okechukwu Onah
Mechanical and production Engineering, Enugu state university of Science and Technology, Enugu State Nigeria.

predict benchmarked FDA result, focuses on transition flow regime of Reynolds number between 2000 and 6500 only. Comparative analysis was for V*elocities,* shear stresses, pressures and jet breakdown location with simulations.

U.S. Food & Drug Administration created an initiative to establish CFD simulation as a regulatory tool for medical scheme. Two 'benchmark 'flow models with specific parameters were tested for providing accurate experimental datasets in the (Stewart, et al., 2012) publication. Experimental results are a useful basis for validating accuracy of CFD simulation and assessing its capacity in development and improvement of medical device. This disquisition focuses on nozzle benchmark model and compares experimental measurement of pressure and velocity provided by Particle image velocimetry (PIV) testing and compares it against CFD results. The ideal medical device made up of four sections: inlet tube, gradual-change section, tube throat and outlet tube. Inlet tube and outlet tube have diameter of 0.012m, throat has a diameter of 0.004m. The cone-shaped "gradual-change" section connects the inlet with throat and has a length of 0.22685m, nozzle has a length of 0.04m. The flow will enter through inlet and then experience a gradual convergence and go through the narrow nozzle throat before it increases at expansion region and flows through the outlet tube. The outlet length is 30 times size of the diameter, 0.36m, which gives enough space for fluid flow full development. The inlet length is calculated using Equation 1.

$$L_e = 4.4D\ Re^{\frac{1}{6}} \quad \ldots\ldots (1)$$

The numerical methodology employed were based on laminar, (www.thermal-engineering.org/what-is-reynolds), where flow rate and tube throat Reynolds number is 500, near transition and turbulent tube throat Reynolds number is 2000 and 6500, used for determination of free stream velocities that allowed calculating first layer height Y^+ (www.cfd-online.com),

CFD, a valuable tool for characterizing flow fields by predicting velocity, pressure, and shear stress using numerical techniques. Over 50 years, CFD application have extended from observing any kind flow around airfoil and automobile to improvement and assessment of blood-contacting devices (Burgree et al., 2001) and (Marsden et al., 2014). The advantages of CFD in designing medical device includes that it provides insight in performance without costly prototypes, providing data assessment at critical regions and predicting difficult measuring quantities which influence blood damage (Raben et al., 2016) and (Fraser et al., 2012). Although U.S. Food & Drug Administration have no CFD simulation need in evaluating blood contacting medical device, but heart valves international standard does (ISO 5840 - 2, 2015) and (ISO 5840 - 3, 2013). (ISO 14708 - 5, 2010) Recognizes Implantable circulatory support device experimental validation with CFD simulation for flow fields characterization in and around these devices, and assess potentials of hemolytic and thrombogenic. (ISO 14708 - 5, 2010) and (ISO 5840 - 2, 2015) standards indicate that CFD usage be limited to design stage which is more appropriate for evaluating relative changes than assessing absolute quantities in design (ISO 14708 - 5, 2010). CFD regulatory tool does not predict value of blood damage. Hence the focus on transitional flow regime of Reynolds number 2000 and 6500. Physical quantities of velocities, shear stresses, pressures and jet breakdown location are compared with simulations. Furthermore, insight into questions like when, where, whether, and how Re transition flow is provided

Hence the focus is on transitional flow regime and thus Reynolds numbers 2000 and 6500 are only analyzed. Physical quantities like velocity, shear stress, and pressure and observations like the jet breakdown location are compared from experiments and simulations. Furthermore, insight into questions like when (Re), where (locations), whether, and how of flow transition is provided.

To evaluate the current state of CFD use, computational studies open to anyone were performed on each model using FDA-specified test conditions. Particle image velocimetry (PIV), CFD, and hemolysis testing results from the first study on the nozzle model have previously been disseminated through a series of publications. (Stewart, et al., 2012); (Stewart et al., 2013); (Hariharan et al., 2011) and (Herbertson et al., 2015). The primary goal of this thesis is to summarize the FDA initiative and to report recent findings from the second benchmark study using the blood pump model by the evaluation of CFD performance using nozzle benchmark of 2D- axisymmetric model based on simulation models.

2 Material and methods

The materials for this study were geometry of the nozzle benchmark model, computer, Ansys fluent simulation, the flow conditions at inlet for the laminar flow (Re=500), transitional flow (Re =2000), and the turbulent flow (Re=6500). The various turbulence models used to resolve the fluid flow were 7 in total: the k-ω model, k-ω SST model, Spalart Allmaras model, Transition SST model, laminar model, k-ε model and Reynolds Stress model. The k-ε and Reynolds Stress model has a y+ value of 30 and the rest of the turbulence models has y+ value as was given in Equation (1)

Table 1 Flow Conditions in the nozzle model

Flow rate (m3/s)	Inlet Re	Throat Re	Inlet velocity u0	Freestream velocity
5.21×106	167	500	0.0461 ms-1	0.4143 m/s
2.08×105	667	2000	0.1842 ms-1	1.6572 m/s
6.77×105	2167	6500	0.5985 ms-1	5.3859 m/s

The equation used to calculate the velocities is the Reynolds Equation shown as Equation 3 from equation 2 below, and the wall distance is calculated using Equations 3 to 5 and is displayed in Tables 1 and 2.

$$L_e = 4.4D\ Re^{\frac{1}{6}} \ldots\ldots\ldots\ldots\ldots\ldots\ldots\ldots\ldots\ldots\ldots (2)$$

$$R_e = \frac{\rho U_{freestream} L_{boundary\ layer}}{\mu} \ldots\ldots\ldots\ldots\ldots (3)$$

$$C_f = (2log_{10}(Re_x) - 0.65)^{-2.3}\ for\ Re_x < 10^9 \ldots\ldots\ldots\ldots (4)$$

$$\tau_w = C_f.\frac{1}{2}\rho U_{freestream}{}^2 (4)$$

$$U_* = \sqrt{\frac{\tau_w}{\rho}}(4) y = \frac{y^+ \mu}{\rho u_*} \ldots\ldots\ldots\ldots\ldots (5)$$

Table 2 Wall distance according to flow conditions

	Re =500	Re=2000	Re=6500
Wall distance (m) (when y+ =1)	6.8×10^{-5} m	2.2×10^{-5} m	8.1×10^{-6} m
Wall distance (m) (when y+=30)	2.0×10^{-3} m	6.6×10^{-4} m	2.4×10^{-4}m

2.1 Nozzle Benchmark Description

The Description of Nozzle Benchmark Model Design of A 2D-axisymmetric axial nozzle model geometry inlet length of 0.23m and out length of 0.36m, throat 0.04m in Figure1, was created in solid work and imported in the Ansys work bench 2020R1, with incompressible fluid blood.

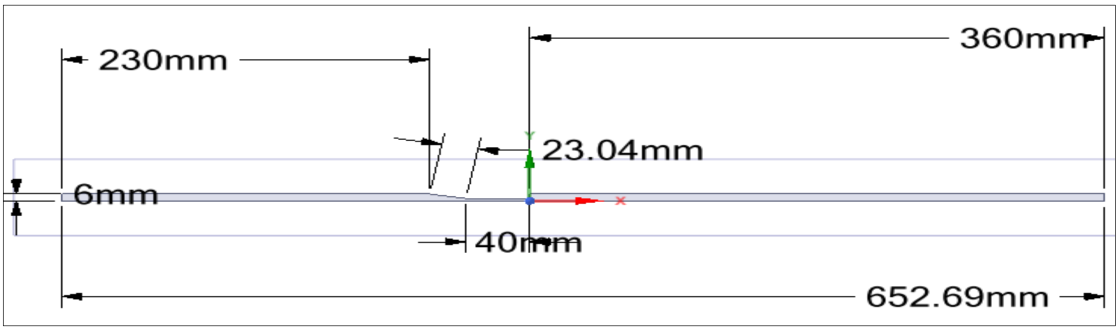

Figure 1 Geometry of 2D axisymmetric axial nozzle model

Then CFD FLUENT SOLVER edge sizing of Figures 2 and 3.

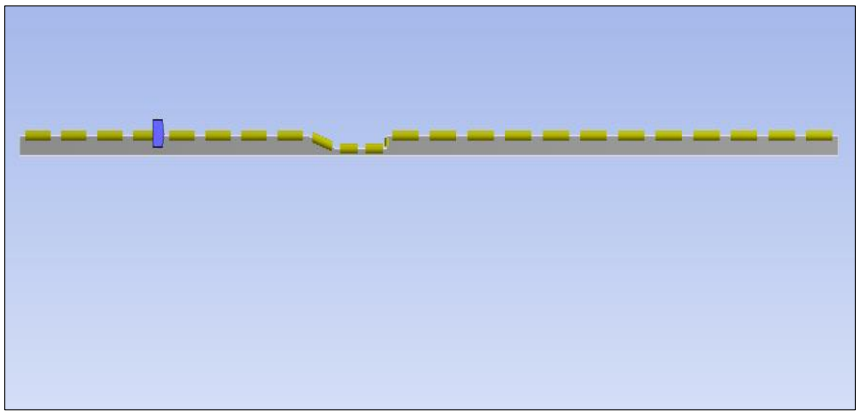

Figure 2 Edge Sizing

Details of "Edge Sizing" - Sizing

Scope	
Scoping Method	Geometry Selection
Geometry	5 Edges
Definition	
Suppressed	No
Type	Element Size
Element Size	Default (3.2636e-002 m)
Advanced	
Behavior	Soft
Growth Rate	Default (1.2)
Capture Curvature	No
Capture Proximity	No
Bias Type	No Bias

Figure 3 Edge Sizing details

2.2 Mesh Generation

Default growth rate used to generate meshes Figures 4 - 6 for each of 0.0008m, 0.0004m and 0.0002m element sizes.

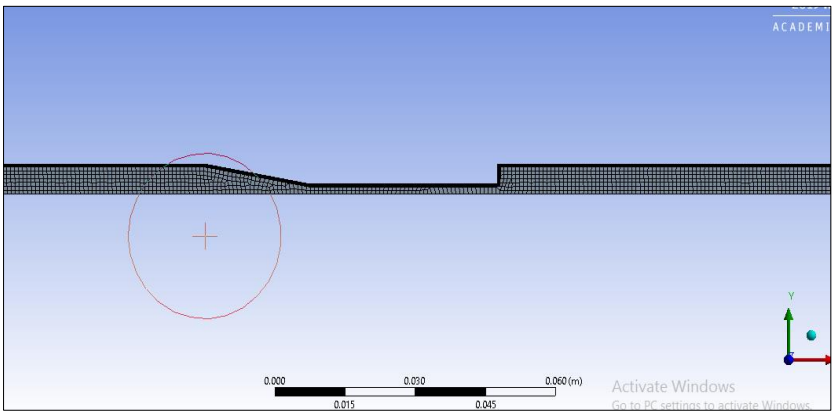

Figure 4 Mesh of element size 0.0008

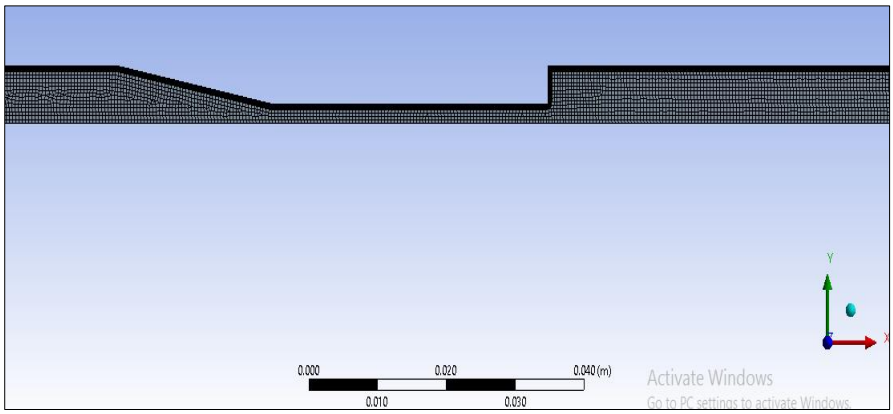

Figure 5 Mesh of element size 0.0004

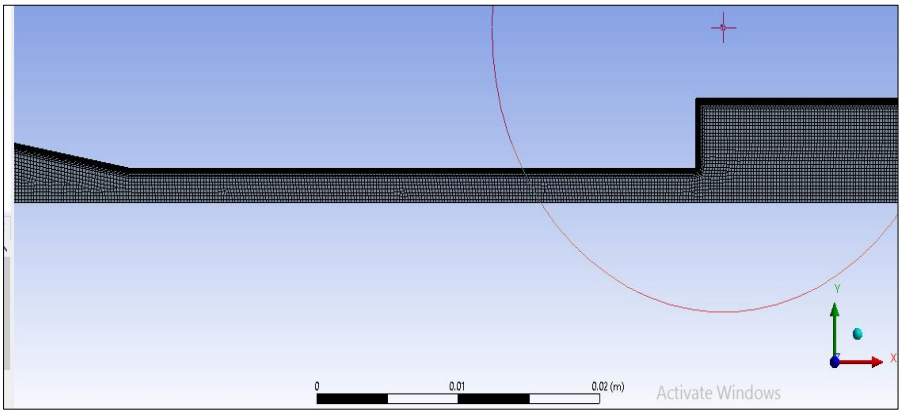

Figure 6 Mesh of element size 0.0002

The next which is set-up was used for the initialization and running calculation for 10000 iterations Figures 7 - 9. The accuracy of the numerical solution presented within this study is contingent on the accurateness of the mesh structure and boundary conditions specified. Mesh convergence is an important part of ensuring that a solution is valid. By monitoring the residual RMS error and ensuring that variables (such as the pressure drop) do not significantly change with the refinement of the mesh. Table 3 shows information about the mesh sizes used when trying to solve the flow problem.

Table 3 Mesh Information

Element Size (m)	Nodes	Elements	Pressure Drop (Pa)
0.0008	13421	12647	21907
0.0004	34610	33169	21512
0.0002	112291	109651	21111

The K-ω SST model was arbitrarily chosen for the mesh independence study and the Reynolds number was chosen to be 6500 with an inlet velocity of 0.5985 ms^{-1}. The convergence criteria were set to $1x10^{-3}$ and a convergence tolerance of 10^{-7} was reached during the hybrid initialization. The residuals were given 1000 iterations to converge and although most of the plots converge around the 10^{-7} and show very good agreement the continuity plot plateaus at around 1.1 $x10^{-3}$ for all the meshes.

2.3 Residual Scale Plot

Figures 7 - 9, thus illustrate the scaled residuals plot at different element sizes. 0.0008 takes 200 iterations to reach a steady-state whereas the other meshes reach a steady-state somewhere around the 150th iteration which is an indication of a higher degree of accuracy.

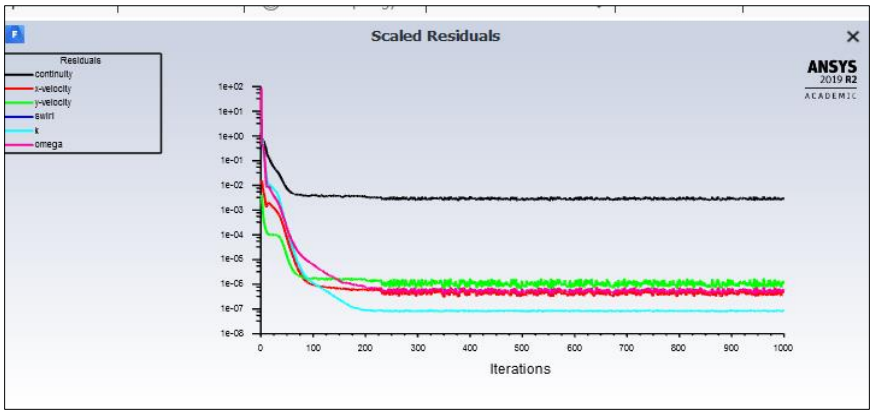

Figure 7 Simulation iteration of Scaled residual value for 0.0004 mesh

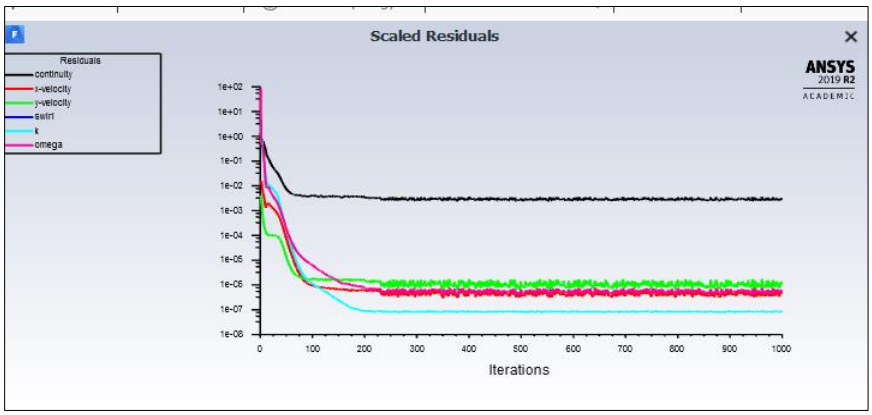

Figure 8 Simulation iteration of Scaled residual value for 0.0004 mesh

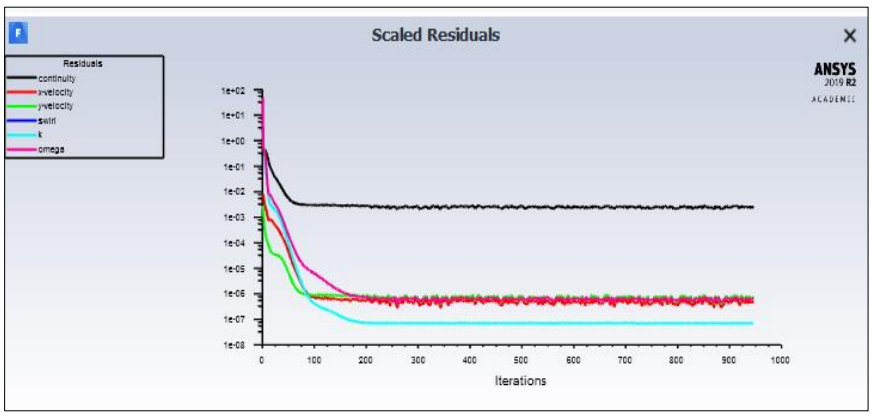

Figure 9 Simulation iteration of Scaled residual value for 0.0002 mesh

3 Results and discussion

The pressure and velocity contours of each element sizes are shown in Figures.10 - 15 respectively. Built on that, the velocity component of element size 0.0008 slowed down at 5.6m//sec is different from the velocities at same point of 0.0004 and 0.0002 element sizes However, velocities at 0.0004 and 0.0002 element sizes started at 6.6m/s and 6.59m/s with 0.01% difference and agreed at velocity 5.9m/sec. Based on the inference, 0.0004 element size was now chosen as a mesh independence for subsequent analysis and simulation for determination of axial velocity at centreline, wall Pressure and axial velocity at different points using K-epsilon, Laminar, K-omega and K -omega-SST models. These effects of these models were studied at before and after the sudden expansion exchange of 0.02m.

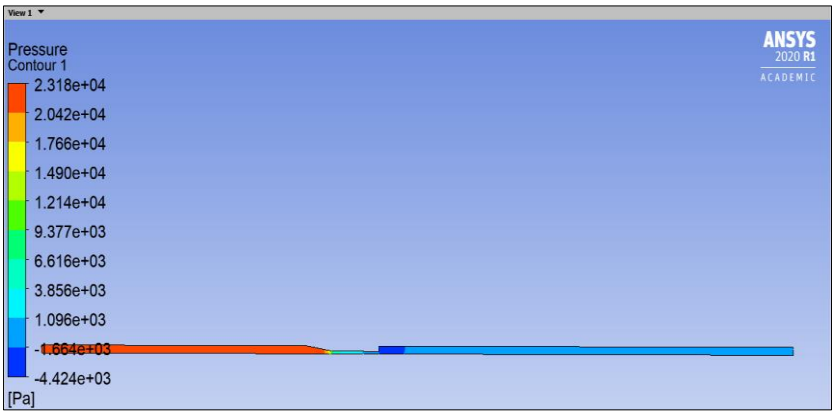

Figure 10 Pressure Contour of 0.0008 element size

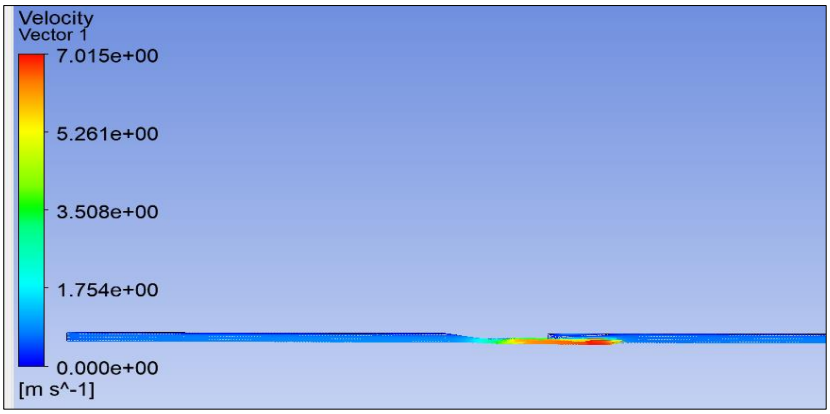

Figure 11 Velocity Contours of 0.0008 element size

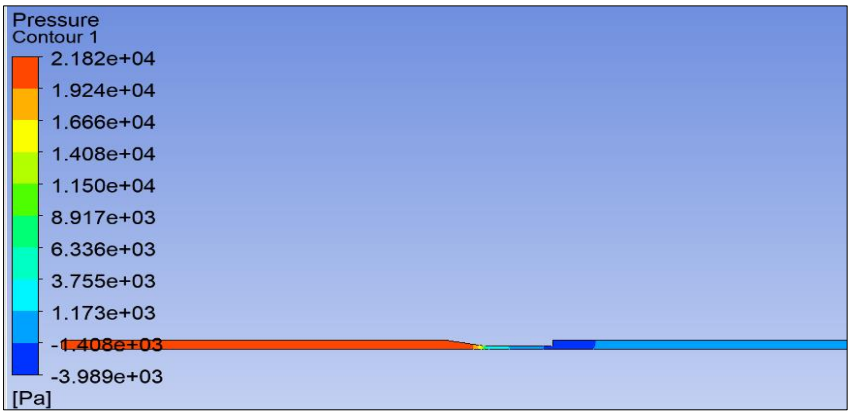

Figure 12 Pressure Contour of 0.0004 element

Table 4 show different flow rates, throat and inlet Reynolds numbers. Table 5 shows Reynolds number and calculated inlet velocities while Table 6 shows the no of elements, nodes, and element sizes and pressure drops.

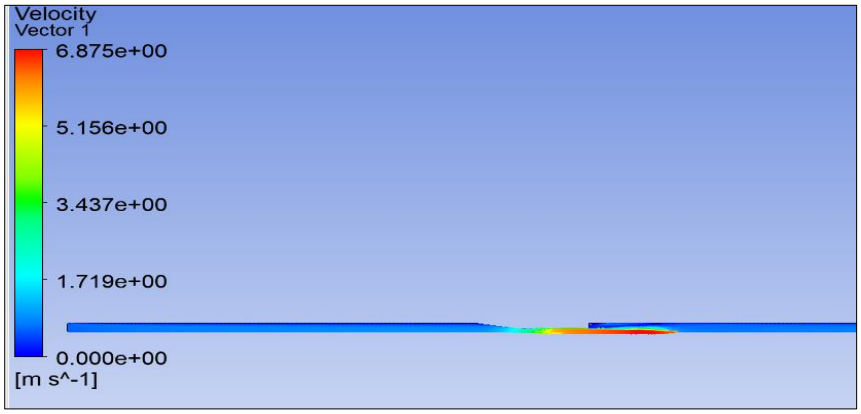

Figure 13 Velocity Contours of 0.0004 element size

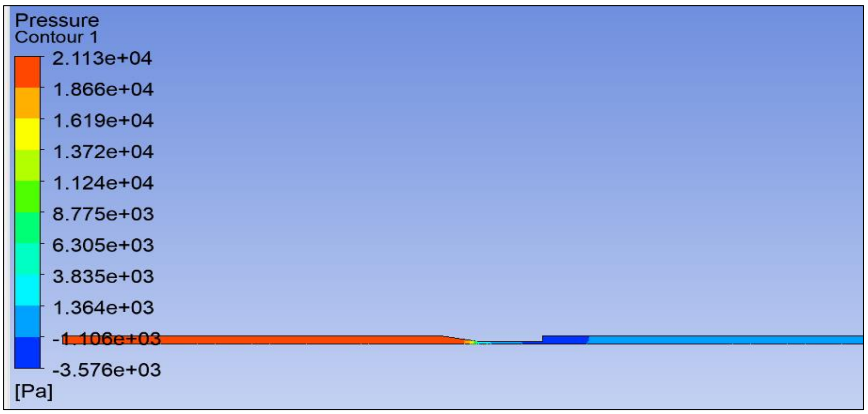

Figure 14 Pressure contour of 0.0002 element size

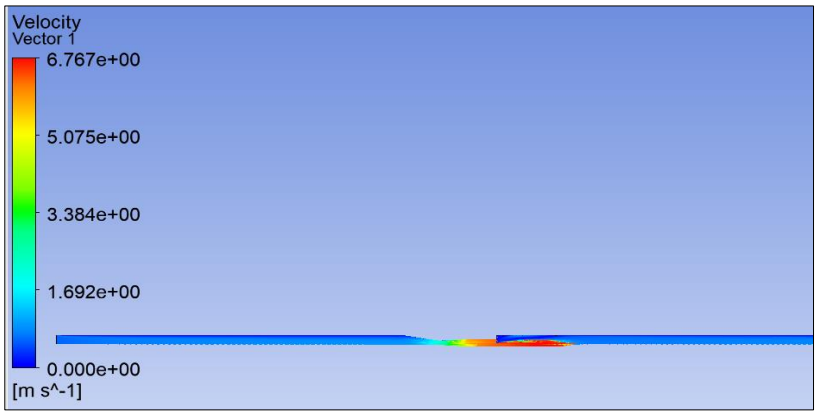

Figure 15 Velocity contours of 0.0002 element size

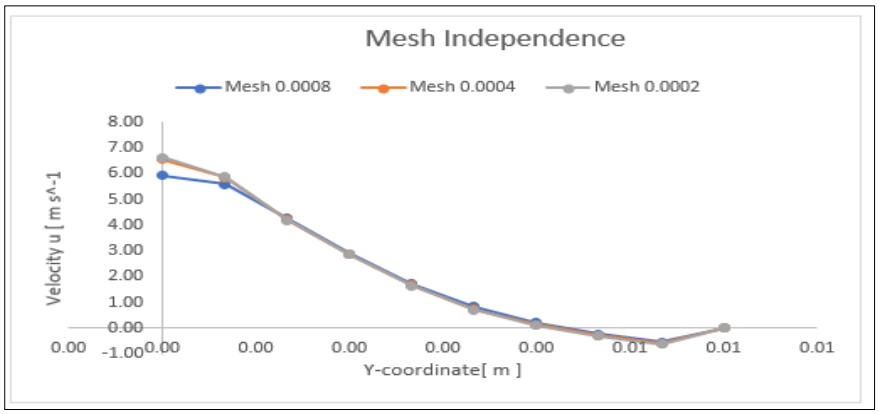

Figure 16 Mesh independence determination

Table 4 Different flow rate throat and inlet Reynolds numbers

Flow Rate (m3/s)	Throat Reynolds Number	Inlet Reynolds Number
5.21 x 106	500	167
2.08 x 105	2000	667
6.77 x 105	6500	2167

Table 5 Reynolds number and inlet velocities

Re	Inlet Velocity (m/s)
6500	0.5985
2000	0.1842
500	0.04613

Table 6 No of elements, nodes, element sizes and pressure drops

No of elements	Nodes	Element Size	Pressure Drop(pa)
16401	17181	0.0008	23132.2
39862	41274	0.0004	21747.4
118394	120986	0.0002	21006.8

3.1 Results of Axial Velocity at Re_{th} = 500

The Models comparative study of axial velocity Re_{th}. of = 500, before sudden expansion at line cut for various Y= -0.088m, -0.048m, and -0.008m with experimental data is presented in Figure 17 as shown

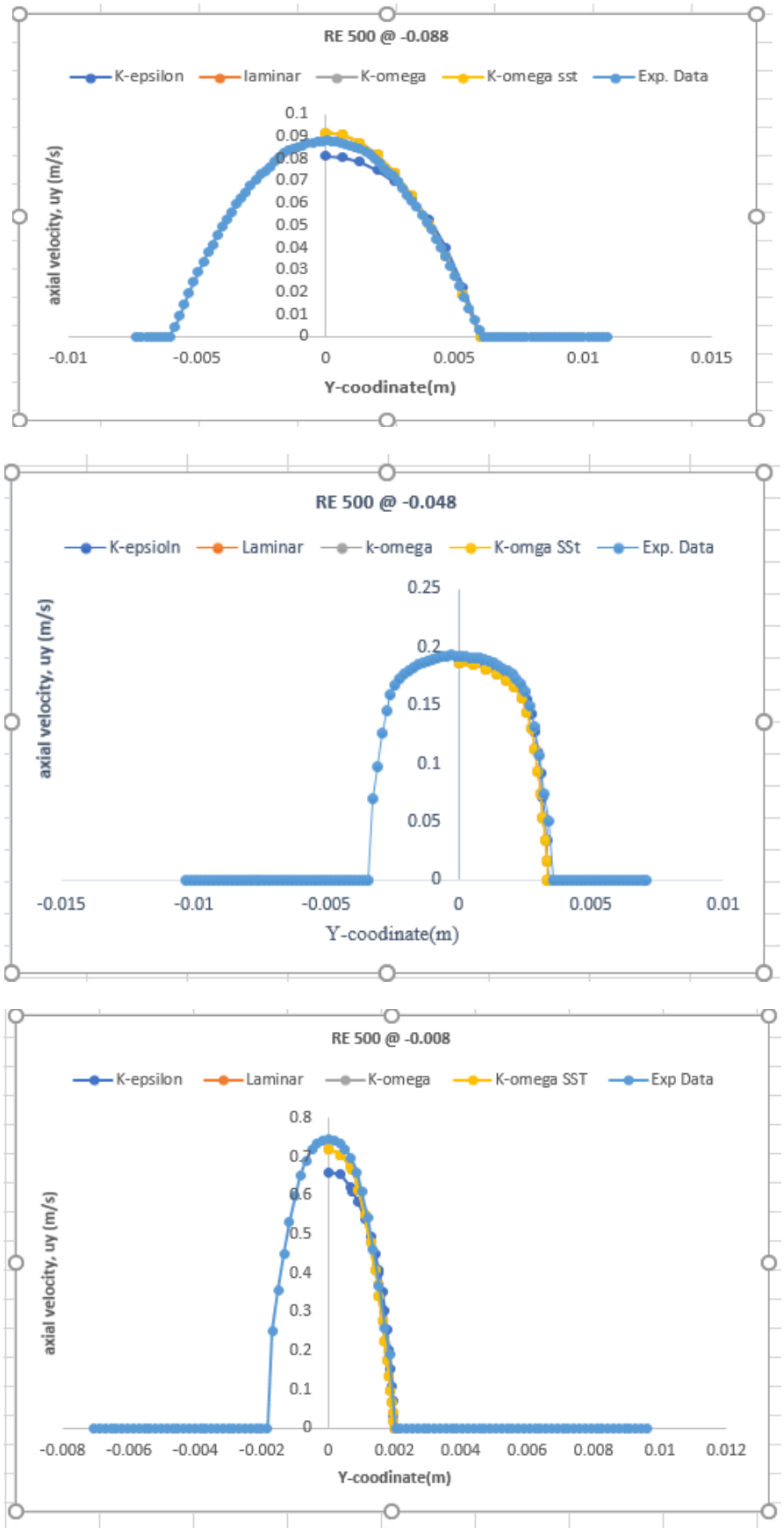

Figure 17 Axial velocity at Re_{th} = 500, before sudden expansion at line cut for various Y= -0.088m, -0.048m, and -0.008m

Figures.17a - c show the simulations of axial velocities Re_{th} = 500 before sudden expansion at Y= -0.088, -0.048, and -0.008. At Figure 17a of -0.008, k-epsilon and K-omega SST deviated from the experimental data plot. However both laminar and K-omega matched the experimental data. Other simulations of Figure 17b and c, showed similar result but with Fig.17c, the K-omega SST and K-epsilon showed deviation from the experimental.

3.2 Results ofAxial Velocity at Re_{th} = 6500

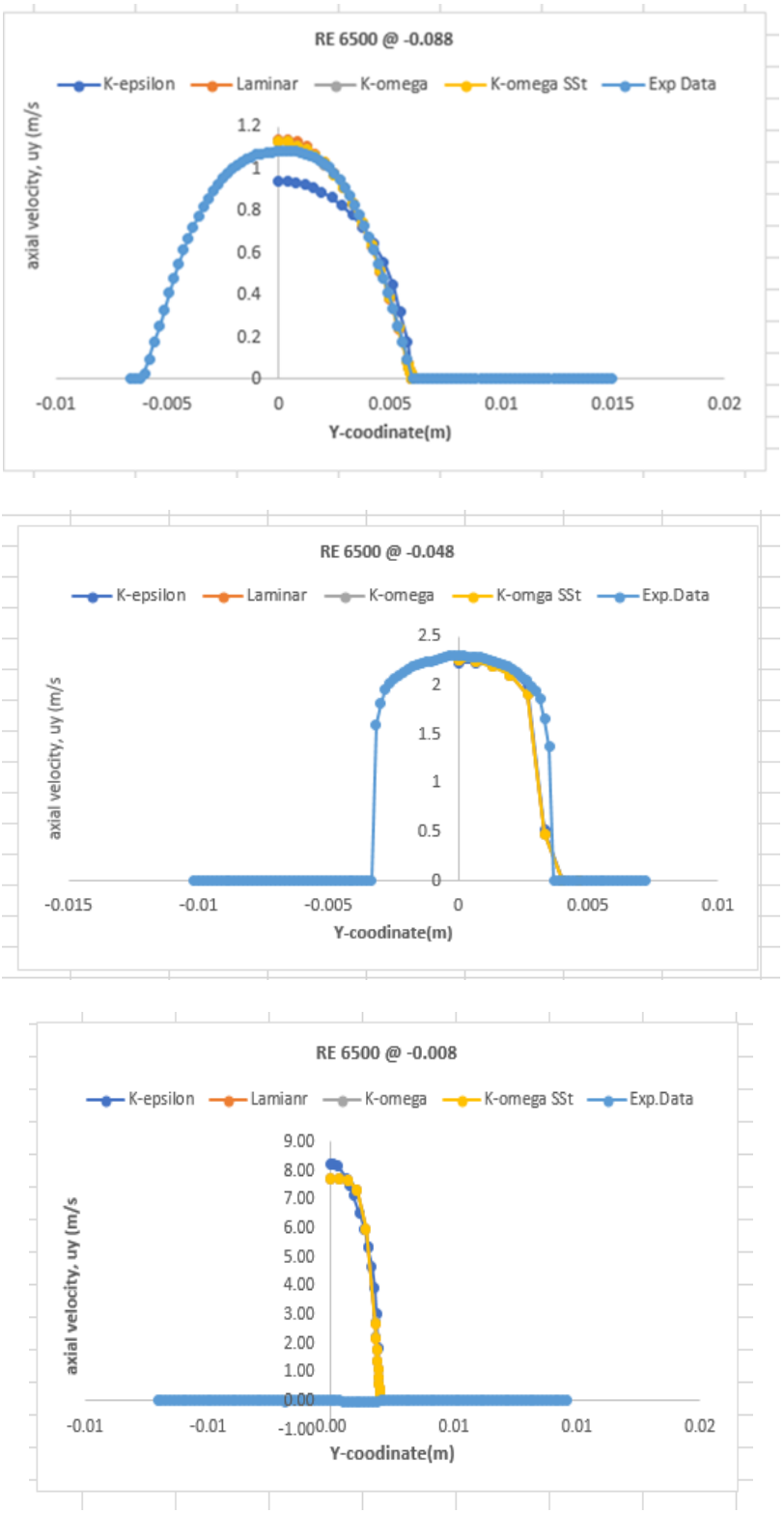

Figure 18 Axial velocity throat at Ret. = 6500, before sudden expansion at line cut for various = -0.088m -0.048m, and -0.008m

The models comparative study axial velocity at $Re_{th.}$ = 6500, before sudden expansion at line cut for various Y = -0.088m, -0.048, m and -0.008m with experimental data is shown in Figure 18 as shown.

Figures 18a - c show the axial velocity throat Reynolds number $Re_{th.}$ = 6500, before sudden expansion at line cut for various Y = -0.088, -0.048, and -0.008. The simulations show that the laminar and K-omega model collapsed and disappeared. This could be the fact that these models are not adopted at higher Reynolds number. The outstanding simulations using turbulence models could not match experimental data downstream of the sudden expansion, with the KE model performing the least well. This is no surprising, because the KE model was developed for high Reynolds numbers and would be expected to be "adjusted" for higher rates of turbulent dissipation than the KO and SST models. For this, turbulent model for this Re_{th} may have been the self-confidence that jets issuing from a sudden expansion are turbulent. The boundary between the jet and recirculated zone represented a sincere uncertainty, but was observed no visible breakdown at Re_{th} = 500 in the experiments. Obviously, at this low Re_{th}, simple turbulence models ought not to be used.

Table 7 Percentage of error for Wall Pressure at Inlet (-0.009m)

Flow conditions	Maximum Difference at -0.09m
Laminar Flow (Re =500)	19.0%
Transitional Flow (Re=2000)	17.2%
Turbulent Flow (Re=6500)	8.10%

4 Conclusion

A 2D-axisymmetric axial nozzle model geometry of faces 0.006m, edges of inlet length of 0.23m, out length of 0.36m, throat 0.04m, and slant length of 0.02304m and axis of 0.653 was created in solid work and imported in the Ansys work bench 2020R1. Four simulation models of laminar, k-omega, k-omega SST and k-epsilon based on inlet throat $Re_{th.}$ = 500, 2000 and 6500 were employed. The K-omega SST was used for mesh independence determination for 0.0008, 0.0004 and 0.0002 element sizes. The element size 0.0008 showed velocity of 5.6m/sec. Element sizes 0.0004 and 0.0002 started at 6.6m/s and 6.59m/s respectively with 0.01% difference and agreed at velocity 5.9m/sec. However, 0.0004 element size was chosen upon subsequent simulation for axial velocity at centreline, wall Pressure and axial velocity at different determinations.

This converged at 0.0002 mesh independence at 2% of total pressure drop. However, 0.0004 was chosen upon subsequent simulation for axial velocity at centreline, wall Pressure and axial velocity at different determinations plots. The axial velocity at centreline for Re_{th} = 500, 2000 and 6500 at line X =0, showed that laminar model is better at lower Reynolds number, followed by transition of Re_{th} =2000, then K-epsilon SST .At Re_{th} = 6500 and inlet Re = 2167, k-epsilon model best matched the experimental data. The axial velocity throat Reynolds number $Re_{th.}$ = 500, after sudden expansion at line cut for various Y = 0.088, 0.024 and 0.08, showed simulations worse match with k-epsilon and K-omega SST, but laminar and K-omega matched with the experimental data, but other simulations showed deviation from the experimental data. The boundary between the jet and recirculated zone represented a sincere uncertainty, but was observed no visible breakdown at Re_{th} =500 in these experiments. Obviously, at this low Re_{th}, simple turbulence models ought not to be used.

Axial velocity at centreline for Re_{th} = 500, 2000 and 6500 at line X =0. The results showed maximum difference of 77.4% for the velocity at centerline at 0.08m and 19% for the wall pressure at -0.09m sudden expansion at laminar region of Re – 500. Besides, 65.6% and 17.2% were obtained at transition of Re =2000, with good agreement between the CFD simulations and the experimental measurements. Nevertheless, at turbulent region Re = 6500, all models were in good agreement at 49.6% velocity centerline and 8.10% pressure drop, except in laminar legion. Downstream of the simulation of Re_{th} =6500, other models disappeared which demonstrated K-epsilon is best at higher Reynolds turbulent region. Categorically, wall pressure showed negligible axial pressure gradient at centerline with drop in normalization point of experimental data from 0 to -120N/m^2 counterbalanced at Re_{th} = 500. This deduction could be drawn by means of differential pressure transducers in some of the experiments data run.

Compliance with ethical standards

Author's contributions

TO write up the manuscript CD and OE conducted the laboratory experiments. TO supervised the laboratory experiment and structured, edited, read, and approved the final manuscript. All authors read and approved the final manuscript.

Funding

No funding was obtained for this study.

Availability of data and materials

The datasets supporting the conclusions of this article are included within the article.

Disclosure of conflict of interest

The authors declare that they have no competing interest.

References

[1] Bernsdorf, J., Harrison, S. E., Smith, S. M., Lawford, P. V., & Hose, D. R. (2008). Applying the Lattice Boltzman Technique to Biofluids: A Novel Approach to Simulate Blood Coagulation. Computation Mathematics Application, (pp. 1408 - 1414).

[2] Burgreen, G. W., Antaki, Z. J., & Wu, A. J. (2001). Holmes: Computational Fluid Dynamics as a Development Tool for Rotary Blood Pump. Artificial Organs, pp. 336 - 340.

[3] Fraser, k. H., Taskin, M. E., Zhang, T., Griffith, B. P., & Wu, Z. J. (2012). A quantitative Comparison of Mechanical Blood Damage Parameters in Rotary Ventricular Assist Device: Shear Stress, Exposure time and Hemolysis Index. Journal of Biomedical Engineering.

[4] Hariharan, P., Giarra, M., & Reddy, V. (2011). Multilaboratory Particle Image Velocimetry Analysis of the FDA Benchmark Nozzle to Support Validation of Computational Fluid Dynamics Simulations. Journal of Biomedical Engineering.

[5] Herbertson, L. H., Olia, S. E., & Daly, A. (2015). Multilaboratory Study of Flow-Induced Hemolysis Using the FDA Benchmark Nozzle Model. artifical organ proceedings, (pp. 237 - 248). arlington.

[6] Huang, I. C. (2018). CFD Validations with FDA Benchmarks of Medical Devices Flows. 15th International LS-DYNA Users Conference. Detroit.

[7] ISO 14708 - 5. (2010). Implant for Surgery - Active Implantable Medical Devices Part 5. arlington, VA, USA.

[8] ISO 5840 - 2. (2015). Cardivascular Implant - Cardiac Valve Protheses part 2. VA, USA.

[9] ISO 5840 - 3. (2013). Cardivascular Implant - Cardiac Vlave Protheses part 3. VA, USA.

[10] Jain , K. L. (2020). Transition to Turbulence in an Oscillatory Flow Through Stenosis. Biomechanics and Modeling in Mechanobiology Proceedings, (pp. 113 - 131).

[11] Jain, K., Ringstad, G., Fide, P. K., & Mardal, K. A. (2017). Direct Numerical Simulation of Transitional Hydrodynamics of the cerebrospinal Fluid in Chiari Malformation: The Role of Cranio-Vertebral Junction. International Journal of Numerical Methods and Biomedical Engineering.

[12] Marsden , A. L., Bazilevs, Y., Long, C. C., & Behr, M. (2014). Recent Advances in Computational Methodology for Simulation of Mechanical Circulatory Assist Devices. Wiley Interdiscipline Revise System Biomedics, (pp. 169 - 188).

[13] Raben, J. S., Hariharan, P., Robinson, R., Malinauskas, R., & Vlachos, P. P. (2016). Time-Resolved Particle Image Velocimetry Measurement with Wall Shear Stress and Uncertainty Quantification for the FDA Nozzle Model. Cardivascular Engineering Technology, (pp. 7 - 22).

[14] Stewart, S. C., Eric, G., Paterson, Greg, W., Burgreen, P., Hariharan, P., & Matthew. (2012). Assesment of CFD Performance in Simulation of an Idealized Medical Device. Results of FDA'S First Computational Inter-laboratory Study.

[15] Stewart, S. C., Hariharan, P., Paterson, E. G., & Stewart, S. C. (2013). Results of FDA'S First Interlaboratory Computational Study of a Nozzle with a Sudden Contraction and Conical Diffuser. Journal of Biomedical Engineering, 374 - 391.

[16] Sun, C., & Munn, L. L. (2008). Lattice -Boltzmann Simulation of Blood Flow in Digitized Vessel Networks. Computation of Mathematics Application, (pp. 1594 - 1600).

[17] White, A. T., & Chong, C. K. (2011). Rotational Invariance in the Three Dimensional Lattice Boltzmann Method is Dependent on the Choice of Lattice. International Journal of Computational Physics, 6367 -6378.

[18] Zhang, J., Johnson, P. C., & Popel, A. S. (2008). Red Blood Cell Aggregation and Dissociation in Shear Flows Simulated by Lattice Boltzmann Method. International Journal of Biomedicals, 47 -55.